Integrating a Traveling Wave Tube into an AECR-U ion source

Michel Kireeff Covo, Janilee Y. Benitez, Alessandro Ratti
Lawrence Berkeley National Laboratory
One Cyclotron Road
Berkeley, CA 94720

Jasmina L. Vujic
Department of Nuclear Engineering
University of California, Berkeley
Berkeley, CA 94720

Integrating a Traveling Wave Tube into an AECR-U ion source

Michel Kireeff Covo, Janilee Y. Benitez, Alessandro Ratti, and Jasmina L. Vujic.

***Abstract*— An RF system of 500W - 10.75 to 12.75 GHz was designed and integrated into the Advanced Electron Cyclotron Resonance - Upgrade (AECR-U) ion source of the 88-Inch Cyclotron at Lawrence Berkeley National Laboratory. The AECR-U produces ion beams for the Cyclotron giving large flexibility of ion species and charge states. The broadband frequency of a Traveling Wave Tube (TWT) allows modifying the volume that couples and heats the plasma. The TWT system design and integration with the AECR-U ion source and results from commissioning are presented.**

I. Introduction

A Traveling Wave Tube (TWT) system was designed to be used with Advanced Electron Cyclotron Resonance - Upgrade (AECR-U) ion source [1] of the 88-Inch Cyclotron at Lawrence Berkeley National Laboratory.

The AECR is optimized for production of highly charged ion beams for the 88-Inch Cyclotron accelerator. Previously, the AECR-U was driven by Klystrons that produced 14.3 and 10.4 GHz heating frequencies. The 10.4 GHz Klystron has been replaced by a TWT with frequency range of 10.75 to 12.75 GHz. The upgrade has the advantage of allowing studies of the AECR-U source efficiency using the TWT broadband frequency microwave tune.

In conventional ECR sources [2], the ECR zones are usually thin annular, ellipsoidal-shaped surfaces which surround the optical axis of the source. The microwave power can only be coupled to the plasma in these zones, which occupy a small percentage of the ionization chamber, leaving the remainder of the plasma chamber as "unheated" zones. The absorvity of the plasma is governed not by the size of the plasma, but by the size of the region of resonance. Through a resonant heating process the microwave radiation accelerates the electrons, which in turn ionize the atoms or molecules present in the plasma through collisional processes.

The AECR-U ion source magnetic field strength was designed for optimized operation at 14 GHz, which is its primary heating frequency for the ECR plasma. In addition, the heating frequency was previously fine tuned to maximize the AECR-U performance for high charge state production. A solid state circuit providing a bandwidth of 100 MHz drove the LBNL AECR-U ion source in the narrow frequency range of 14.2520 to 14.3043 GHz [3]. During these heating tests, the high charge state performance was measured and optimized by small adjustments in the driving frequency, showing a region of maximum absorption for single frequency operation of 14.2713 GHz that coincided with a low reflected power.

The new TWT is aimed to optimize the secondary heating frequency with the goal of further optimizing the AECR-U source performance. The TWT frequency range of 10.75 to 12.75 GHz is chosen to give a secondary frequency that still allows the electrons to resonate with the magnetic field that is set by the primary frequency of 14 GHz. The secondary frequency increases beam production by providing a second resonance surface for electron heating, in addition to improving plasma stability.

Previous TWT studies [4, 5, 6, 7] reported that the use of broadband microwave frequency for electron heating may enhance the performance of ECR ion source. The studies claim that the larger microwave bandwidth increased the ECR heating zone volume, allowing a large area in which electrons can become accelerated, thereby increasing electron temperature and density.

Numerical simulations of the ECR heating show the strong dependence of the excited modes in the plasma chamber [8], and the need for frequency tuning to improve the source performance [9].

This paper describes the design of an RF source, Automatic Gain Control (AGC) unit, interlock and initial results from the commissioning of the TWT system showing ion beam currents extracted and reflected power measurements.

II. Controller Design

The TWT control chassis is shown in Figure 1. It contains the interlock control, the RF source, and the AGC unit. The interlock control provides the interlock complete signal to the TWT, allowing it to transmit. The RF source has an oscillator circuit that allows sweeping the frequency in the range of 10.75 to 12.75 GHz. The RF source output is connected to a voltage controlled attenuator regulated by the AGC unit. The TWT is configured to have a gain of 50 db, so the output power of the TWT is kept constant by controlling the input power with the AGC. The AGC system has a microprocessed circuit that samples the forward power and provides regulation. The reflected power is also sampled. If it is higher than a threshold, the voltage controlled attenuator is set to the maximum attenuation, shutting down the output power of the TWT.

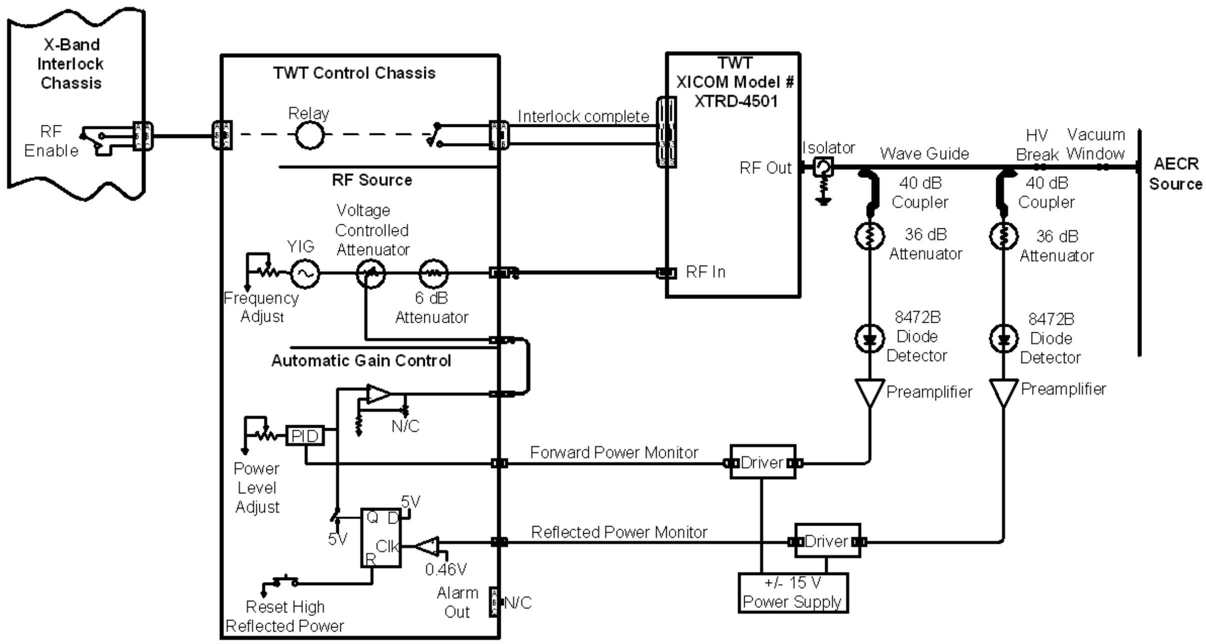

Fig. 1. Simplified block diagram of the system. It consists of a TWT and a control chassis with an RF source, an automatic gain control (AGC), and an interlock control circuitry. The power to the AECR is measured with diode detector and kept constant by controlling the input power to the TWT with the AGC.

A. RF Source

The RF source uses an MCO-0818-500-01 YIG oscillator from Microsource Incorporation. It is a multi-octave Yttrium, Iron and Garnet (YIG) tuned oscillator that ranges from 8 to 18 GHz. It has ~20 MHz/mA tuning sensitivity with hysteresis of 4.1 MHz and provides a minimum of 15 dbm output power. The oscillator is heated so the YIG pellet reaches its operating temperature rapidly, but it is assembled over a heat sink so the heat loss generated by the main tuning coil is cooled.

A precision current source is used to control the frequency. The circuit is configured as a return-line current sensing control with a 1 Ω sensing resistor, which is a precision power resistor with a low temperature coefficient of resistance. The analog voltage across the resistor is digitalized by A/D module of 16F877 PIC microprocessor and displayed in the LCD interface module. The 10 bits A/D module gives 0.1% error of the measured frequency. It corresponds to only 10 MHz for each 10 GHz and is considered negligible for the experiments.

The frequency is calibrated with a microwave frequency counter. A spectrum analyzer shows an RF signal spectrum with a narrow bandwidth of ~ 8 MHz (FWHM). The YIG oscillator output is connected to the voltage controlled attenuator, VVAN-8018-60, from American Microwave Corporation that has a frequency range of 8.0 to 18.0 GHz with a 10 db/Volt analog transfer function. The attenuator is linearized to 0.1% with typical insertion loss of 2.7 db and it is controlled by the AGC circuit.

The RF source output feeds the TWT, model XTRD-4501, that has the electrical specifications of 450W output power and 10.75-12.75 GHz frequency range. In order to protect the tube preamplifier, the RF source frequency was limited to the TWT frequency range.

Because the TWT is 10 meters away the RF source, a low loss cable, model UFB311A from Micro-Coax Company, is used, resulting in an insertion loss of ~6.9 db. Although the insertion loss is high, the RF power loss is low because the YIG oscillator provides only ~15 dbm.

As the TWT is set to the maximum gain of 50 db, further 6 db attenuation is added to avoid the TWT from reaching saturation at 56.5 dbm.

B. Automatic Gain Control

An accurate leveling of the power is necessary in order to ensure the AECR-U plasma stability. Therefore an Automatic Gain Control (AGC) is designed to control the input power to the TWT, keeping the output power at a constant power level.

The TWT has reflected power protection of ~49 dbm. A customized WR-75 circulator of high power from Apollo Microwaves is placed next to the TWT output to provide secondary protection.

The TWT signal is attenuated 40 db by a directional crossguide and attenuated another 36 db, giving a maximum signal of -20dbm. At this power level the 8472B low barrier Schottky diode detector is in the square-law region, where its output voltage is proportional to the input RF power.

As the maximum diode detector voltage output is only a few milivolts, the signal needs to be preamplified before it is transmitted to the AGC unit. The precision variable gain DC voltage amplifier, model 351A-1-4.7-NI, from Analog Modules Corporation is chosen as a preamplifier because of the low noise and 20-40 db adjustable gain, allowing amplification of the signal to few volts. As the AGC unit is 10 meters away from the diode detectors, a driver was designed

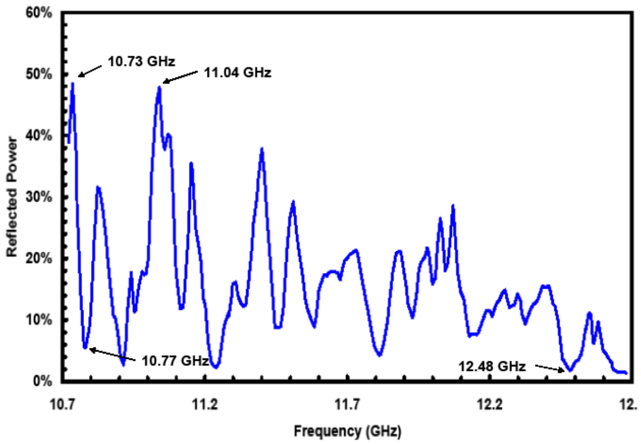

Fig. 2. Percentage of power that is reflected versus frequency with plasma. Sudden variations of plasma coupling are obtained with small variations of frequency. The frequencies 10.73 and 11.04 GHz have high reflected power and the frequencies 12.48 and 10.77 GHz have low reflected power.

and installed after the preamplifier.

The AGC is a microprocessor board utilizing two 16F877 PIC ICs. One is dedicated to sample and display the value in a LCD interface module. The other regulates the power output. An auxiliary protection circuit automatically disables the output power in case of high reflected power failure, set to ~70W. It bypasses the microprocessor logic and provides full attenuation. The circuit was set to give a delay of 35 miliseconds in order to avoid false triggers during the RF frequency adjustments.

PID Controller Algorithm

The step response of a TWT has the rise time of 10 to 20 ns [10] and is assumed instantaneous. The TWT system is modeled as a state machine, so the dedicated microprocessor corrects the output power using a PID algorithm [11], described below. The previous_error variable saves the preceding error variable before the new error is calculated. The power measured (val2) and a power requested (val1), which corresponds to a voltage of the diode detector and the voltage level adjusted with a potentiometer respectively, are measured by internal A/D modules of the 16F877. The algorithm calculates the error variable and the proportional (P), derivative (D), and integral (I) terms. The variable error is obtained from the difference between the power requested and the power measured. The proportional term is obtained by multiplying error by a constant Kp. The derivative term is obtained by multiplying error-previous_error by a constant Kd. The integral term is obtained by adding the previous integral term I to the error and then multiply by a constant Ki. The integral term is limited to a factor of 0.5 in order to avoid wind up. The digital output variable that is the sum of these three terms (P+D+I) is converted to an analog output voltage and applied to the voltage controlled attenuator that regulates the power level.

$$
\begin{aligned}
&previous\_error = error;\\
&error = val2 - val1;\\
&P = Kp * error;\\
&D = Kd * (error - previous\_error);\\
&I = I + Ki * error;\\
&if\ \ (I > 0.5)\ I = 0.5;\\
&if\ \ (I < -0.5)\ I = -0.5;\\
&output = P + D + I;\\
&if\ \ (output > 5)\ output = 5;\\
&if\ \ (output < 0)\ output = 0;
\end{aligned}
$$

PID algorithm

Simulation of the state machine provided initial coefficients of Kp = 0.5, Kd = 0.05, and Ki = 0.1. The PID filter is tuned by applying a step function and adjusting the overshoot term, caused by the proportional term, and the response settling time, caused by the integral term. The derivative term is kept low to avoid possible noise oscillations, but keeping the ability to correct large sudden changes. After bench tuning, the optimal coefficients are Kp = 0.65, Kd = 0.05, and Ki = 0.1. The PID response to a 1 Volt step applied to the AGC unit on bench has rise time of 40 ms with 12% overshoot and 350 ms settling time.

C. *Interlock*

The TWT control chassis is connected to the X-band interlock chassis that receives signals from the redundant interlock chain, Figure 1.

The “RF enable” is on if the safety and source interlocks are complete. The safety interlock protects the operators so they cannot come into contact with high voltage, high current, or RF. It is made up when the doors are locked, and the high voltage cages and the door keys are in place.

The source interlock ensures that the source is operated under appropriate conditions to make plasma, which is the load for the RF power produced. The conditions are that the chamber vacuum should be low and the magnets, the high voltage, and the cooling system should be turned on.

When the “RF enable” is on, a relay will close contact informing the TWT that the interlock is complete, so the system is allowed to transmit. If during the transmission the redundant interlock chain trips off, the relay will open and the TWT interlock will stop the transmission and an alarm will sound.

III. TWT COMMISSIONING

During the following measurements to check the system functionality, an oxygen plasma is optimized to obtain maximum ion beam current of the charge state O^{+7} by setting the TWT forward power to 30W and varying the magnetic confinement fields, the input oxygen gas pressure, and the bias disk voltage. The percentage of power that is reflected versus the frequency, Figure 2, is obtained without changing the optimized parameters. As can be seen, sudden variations of plasma coupling can be obtained with small variations of frequency, similar to results observed in [12].

The measurements were taken by changing the frequency and reading the forward and reflected power. The precision current source - section II.a, which is used to control the frequency of the YIG oscillator, was temporarily computer-controlled by LabVIEW, using an analog voltage output from a National Instruments card.

Concurrently the forward and reflected power monitor voltages were recorded. The reflected power percentage was obtained by dividing the reflected power by the forward power.

The frequencies 12.48, 10.77, 10.73, and 11.04 GHz have reflected power of 1.7%, 5.7%, 48%, and 49%, respectively. Assuming that good plasma coupling results in less reflected power, it is possible to compare the charge-state distributions in order to see if the power is being absorbed by the plasma.

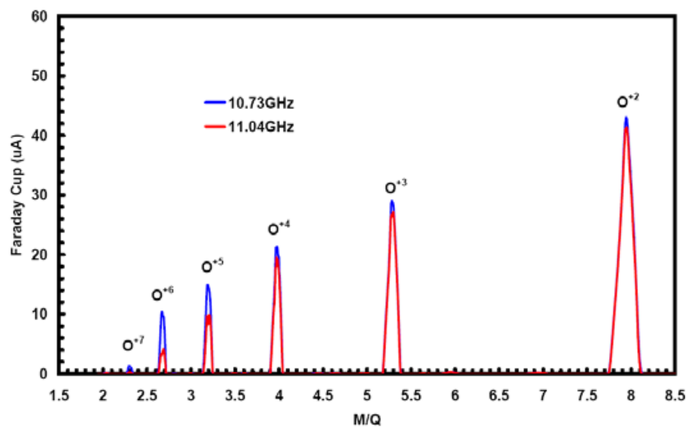

(a)

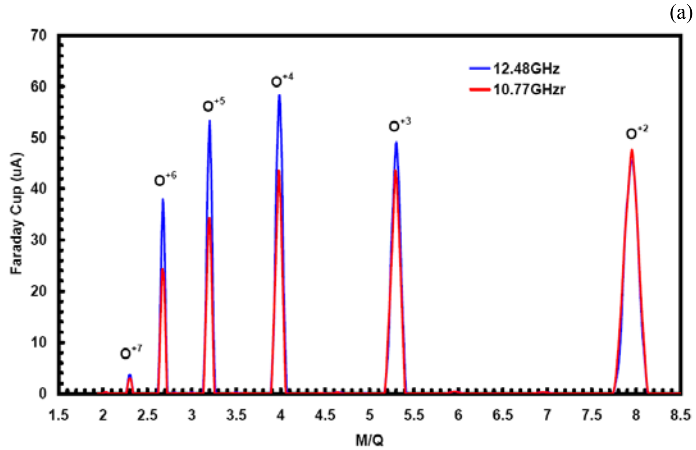

(b)

Fig. 3. Oxygen Charge-State Distribution. (a) at High Reflected Power. (b) at Low Reflected Power. Higher charge-states are enhanced at lower reflected power, showing a better plasma coupling and heating.

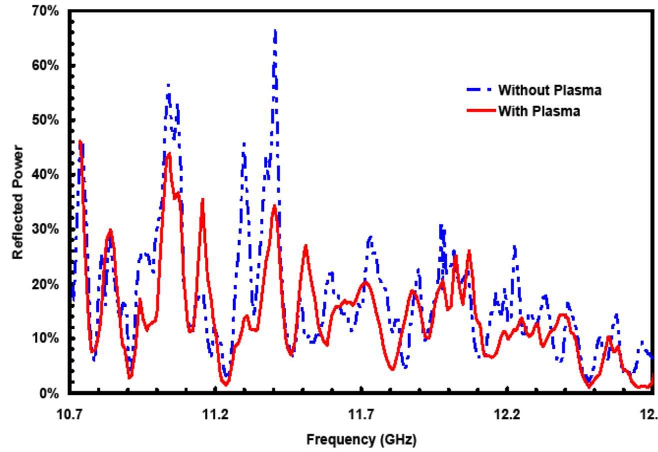

Fig. 4. Percentage of power that is reflected versus frequency with and without plasma. Power matching varies when the frequency changes and sometimes is worst in the presence of plasma.

Figure 3a shows the charge state distribution peaking at O^{+2} for the 10.73 and 11.04 GHz frequencies in which high reflected power is measured. Figure 3b shows the charge state distribution peaking at O^{+4} for the 12.48 and 10.77 GHz frequencies in which low reflected power is measured.

The higher charge-states are enhanced at lower reflected power, Figure 3b, confirming a better plasma coupling and heating.

Figure 4 shows an independent set of measurements of the percentage of forward power that is reflected in the presence and absence of plasma using the same methodology described above. A Faraday cup located after the AECR extraction was used to confirm the presence of plasma during the solid red line measurements. In order to assure the absence of plasma during the blue dashed line measurements, no gas was leaked and the axial magnetic field, provided by two sets of solenoids, was turned off.

The percentage of reflected power with the presence of plasma is consistent with previous measurements from Figure 2. Most of the time the reflected power is higher without plasma, but at some frequencies the reflected power is higher with plasma. The plasma is a dispersive medium having anisotropic inhomogeneity [13], resulting in different distribution of electric permittivity for different frequencies and consequently varying the relative spatial distribution of electrons and ions. As a result, the plasma-cavity impedance and power matching vary when the frequency changes, consequently in some conditions the mismatch observed with the reflected power could be higher in the presence of plasma. This phenomenon is not taken into account in Geller's scaling laws [14] that assume a dependence of the square of the feeding frequency.

IV. Conclusion

A broadband 10.75 to 12.75 GHz TWT was successfully installed at the AECR-U ion source at the 88-inch Cyclotron at Lawrence Berkeley National Laboratory. It allows optimizing the high charge state performance of the AECR-U by tuning the secondary heating frequency. An RF source and AGC unit were constructed, integrated and interlocked with the AECR-U system. In order to maintain the plasma stability, a PID algorithm keeps the output power level constant by regulating the input power that feeds the TWT.

Measurements resulting from the commissioning were performed at the same magnetic field strength, gas pressure, and bias disk voltage. The TWT RF power couples with plasma until the plasma density reaches the critical value at which the plasma, excitation, and electron cyclotron frequency are equal. Standing waves persist after the plasma ignition, generating strong inhomogeneities in electric field distribution where the wave-particle energy transfer occurs. Faraday cup current and reflected power measurements show sudden variations of plasma coupling can be obtained with small variations of frequency.

Acknowledgment

The authors want to thanks Daniela Leitner and Claude Lyneis for the thoughtful comments and suggestions.

This work was supported by the Director, Office of Science, Office of High Energy and Nuclear Physics, Division of Nuclear Physics, US Department of Energy under Contract No. DE-AC02-05CH11231.

References

[1] C. M. Lyneis, Z. Q. Xie, D. J. Clarck, R. S. Lam, and S.A. Lundgren, in: Proceeding of the 10th International Workshop on ECR Ion Sources, Oak Ridge, ORNL CONF-9011136, 1990, p. 47.
[2] G. D. Alton and D. N. Smithe, Rev. Sci. Instrum. 65 4 (1994) 775.
[3] M. Galloway, D. Leitner, C. M. Lyneis, and W. Cornelius, High Energy Physics 31 (2007) 75.
[4] G.D. Alton, Nucl. Instr. & Meth. A 382 (1996) 276.
[5] S. Gammino, G. Ciavola, and L. Celona, Nucl. Instr. & Meth. A 491 (2002) 342.
[6] A. Galatà et al., “Comparison of ECR ion source performance for different microwave generators,” INFN/TC-04/04 report, March 19, 2004.
[7] O. Tarvainen, et al., Nucl. Instr. & Meth. A 261 (2007) 1044.
[8] S. Gammino et al., "Numerical Simulations of the ECR Heating With Waves of Different Frequency in Electron Cyclotron Resonance Ion Sources," IEEE Trans. Plasma Sci. , vol.36, no.4, pp.1552-1568, Aug. 2008.
[9] F. Consoli et al., “Microwave fields distribution and ECR heating process,” Rev. Sci. Instrum., vol. 79, no. 2, p. 02A 308, Jan. 2008.
[10] Brian D. May, Pulsed response of a traveling-wave tube, NASA technical memorandum 103672, January 1991.
[11] Aidan O’Dwyer, Handbook of PI and PID Controller Tunning Rulles (Imperial College Press, London, 2003).
[12] L. Celona, et al., Rev. Sci. Instrum. 79 (2008) 023305.
[13] V. Toivanen, Rev. Sci. Instrum. 81 (2010) 02A319.
[14] R. Geller et al., Proc. 8th workshop on ECRIS, East Lansing, MI, 1987, p.1.